

Effect of Advance Ratio and Blade Planform on the Propeller Performance of a High Altitude Airship

Z. Liu, P. Liu[†], Q. Qu and T. Hu

Beijing University of Aeronautics and Astronautics, Beijing, 100191, China

[†]Corresponding Author Email: lpq@buaa.edu.cn

(Received June 23, 2015; accepted February 20, 2016)

ABSTRACT

Experimental investigations on the influences of Reynolds number, blade planform and advance ratio on the aerodynamic performance are carried. Different from conventional aircraft propellers, the HAA propellers are characterized by low Reynolds number, large thrust requirement and low advance ratio. At the moment, the theoretical guidance and industrial experience in designing such propellers are still lacked. In the present study, the influence of Reynolds number is firstly studied via tests of a propeller at different rotational speeds. It is found that, for the propeller with airfoil S1223, the influence of Reynolds number is negligible as $Re_{0.7} > 1.2 \times 10^5$ ($Re_{0.7} = 0.7\rho\pi n_s D b_{0.7}/\mu$). The tests regarding the influences of blade planform and advance ratio on propeller performance are carried in the condition of $Re_{0.7} \geq 1.5 \times 10^5$. The results show that, when advance ratio is below 0.8, the blade with narrow tip is favorable to the propulsive efficiency. Hence, it is suggested that the blade with narrow tip should be adopted by the large thrust and small advance ratio HAA propellers. For HAA propellers with advance ratio greater than 0.8, the propulsive efficiency can be benefitted by increasing the blade tip width. Hence, the blade with wide tip is more suitable in this application.

Keywords: High altitude airship propeller; Blade planform; Low Reynolds number; Low advance ratio.

NOMENCLATURE

A	$\beta + \gamma$, sum of interference angle and drag-lift angle	r	radius to propeller blade element
AF	$\frac{10^5}{16} \int_{0.2}^1 \frac{b}{D} \left(\frac{r}{R}\right)^3 d\frac{r}{R}$, activity factor	R	radius of propeller
b	chord length of local blade element at r	Re _{0.7}	$V_s b_{0.7}/\nu$, Reynolds number of propeller based on chord length at $r/R = 0.7$
C	thickness of blade of blade element	T	thrust of propeller
C _L	airfoil lift coefficient	UAV	unmanned aerial vehicle
C _P	propeller power coefficient	V	advance velocity of propeller
C _T	propeller thrust coefficient	V _s	$0.7\pi D n_s$, tangential speed at $r/R = 0.7$
C _X	universal dimensionless parameter	α	attack angle of blade element
CR	$b_{1.0}/b_{0.45}$, chord ratio	β	interference angle
D	diameter of propeller	γ	$\arctan(C_D/C_L)$, airfoil drag-lift angle
HAA	high altitude airship	η	propeller propulsion efficiency
Mar	tip Mach number	θ	blade twist angle
n	propeller rotational speed	$\Delta\theta$	$\theta_{0.2} - \theta_{1.0}$, difference of blade twist angle
n _s	propeller rotational speed (revolutions per second)	λ	$V/n_s D$, advance ratio
N _B	number of blade	ν	kinematic viscosity
P	power of propeller	ρ	density of air
Q	torque of propeller	φ_0	$\arctan(V/2\pi n_s r)$, airflow angle
		$\chi_{0.7}$	pitch angle at $r/R = 0.7$

Table 1 Propeller parameters of different vehicles

Type	Conventional aircrafts		UAVs		HAAs	
Vehicle	C-130	Y-8	Colozza (2003)	Koch (1998)	Beemer (1975)	Okuyama <i>et al.</i> (2006)
Altitude, km	6.1	8.0	30.0	25.9	21.0	18.0
Fly speed, m/s	194	153	130	118	8.18	16
Thrust, N	--	11005	35	450	120	234
Rotational speed, rpm	1021	1075	1172	848	75	450
Diameter, m	4.1	4.0	2.8	4.6	10.4	4.2
Number of blade	4	6	6	3	3	3
Advance ratio	2.78	2.13	2.37	1.81	0.63	0.51
Propulsive efficiency	--	0.87	0.85	0.85	0.78	0.69

1. INTRODUCTION

With advantages of long-time and fixed-point residence in space, high loading capacity, high recyclability, low energy consumption and low cost, a high altitude airship (HAA) has huge potential in both civil and military applications. Thus, it has become a hot issue of the modern aerospace sciences (Mueller *et al.* 2004; Brooke 2005; Schmidt *et al.* 2007; Alam *et al.* 2013).

The typical mission altitude of a HAA is within the range of 20 - 22 km, where the wind speed is less than 24.5 m/s (Pancotti 2009). Coupled with the greater kinematic viscosity ($1.61 \times 10^{-4} m^2 / s$, 10 times larger than that on the ground) at fly altitude, the Reynolds numbers $Re_{0.7}$ of the HAA propellers are relatively small ($Re_{0.7} \sim 10^5$). In order to carry certain weight of payload, the airships are normally designed to be large in size which means large thrust should be provided by the propellers. It is forced to increase either the diameter or the rotational speed of a HAA propeller to gain sufficient thrust. Hence, the advance ratio of a HAA propeller is found significantly smaller than the other vehicles, which is defined as $\lambda = V/nsD$. A list of the propeller parameters of conventional aircrafts, unmanned aerial vehicles (UAV) and HAAs (Beemer 1975; Koch 1998; Colozza 2003; Okuyama *et al.* 2006) are shown in Table 1. It can be seen that, the advance ratios of the conventional aircraft and UAV propellers are greater than 1.5, by contrast, the advance ratios of the HAA propellers are smaller than 1.0. Because the propellers of conventional aircrafts and UAVs have higher cruise speed and larger advance ratio, their propulsive efficiencies are usually greater than 0.85. The cruise speeds and advance ratios of HAA propellers are obviously lower. Consequently, the propulsion efficiencies of HAAs are lower (less than 0.80).

For the design of the conventional aircraft and UAV propellers (high speed and large advance ratio propellers), plenty of theoretical guidance and industrial experience are already exist (Borst 1973; Borst 1973; Mikkelson *et al.* 1984). However, to design the large thrust and low advance ratio HAA propellers, necessary awareness is still lacked, such as the chord length distribution, etc. This situation can be confirmed by the propellers of different HAAs (Beemer 1975; Kim *et al.* 2003; Okuyama *et*

al. 2006; Smith *et al.* 2007) as shown in Fig. 1. It is interested to find that, although these HAA propellers are designed under similar flight conditions, their planforms are dramatically different, which makes the design of such propellers difficult. Thus, the purpose of the present effort is to reveal the influence of advance ratio on propeller aerodynamic performance, find out the appropriate blade planform that is more suitable for the large thrust and low advance ratio HAA propellers and provide experimental basis for the HAA propeller optimization.

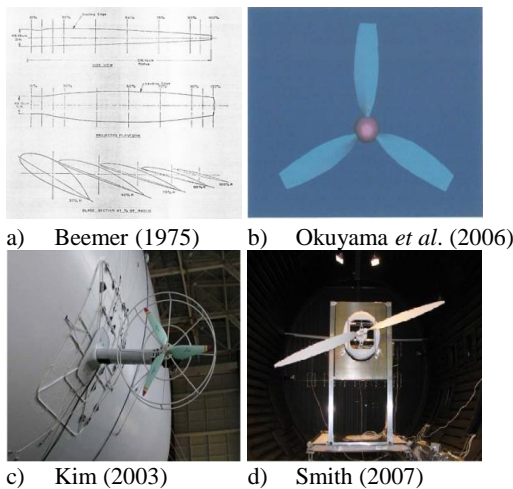


Fig. 1. HAA propellers with different planforms.

According to the similarity theory presented by Liu (2011), for the HAA propellers, the function of propeller performance can be expressed as

$$C_x = f_x (Ma_T, Re_{0.7}, \chi_{0.7}, \Delta\theta, \lambda, \frac{b}{D}) \tag{1}$$

Where C_x is the universal dimensionless parameter which may refer to the thrust coefficient C_T , power coefficient C_P and propulsive efficiency η . It can be seen that the propeller performance is influenced by the tip Mach number Ma_T , Reynolds number $Re_{0.7}$, pitch angle at $r/R = 0.7$ $\chi_{0.7}$, blade twist angle $\Delta\theta$, advance ratio λ and chord length distribution b/D . The influence of Mach number is less significant when the tip Mach number is below 0.85 (Liu 2006). For a HAA propeller, the tip Mach number is generally below 0.65 for its low cruise speed. Although the propeller performance can be

influenced by the low Reynolds number effect (Brandt 2005; Merchant *et al.* 2006; Brandt *et al.* 2011), it has been found by Bass (1986) that the influence of Reynolds number is negligible when the $Re_{0.7}$ is larger than the critical Reynolds number for propellers. The pitch angle (at $r/R = 0.7$) $\chi_{0.7}$ and blade twist angle $\Delta\theta$ are determined by the design advance ratio (Liu 2006). Hence, the overall performance of a HAA propeller is determined by the advance ratio λ and chord length distribution b/D as shown in Eq. 2.

$$C_x = f_x\left(\lambda, \frac{b}{D}\right) \quad (2)$$

Similar study was carried by Hartman (1938) who conducted tests on four aircraft acicular propellers (wide middle section, narrow tip and root) that were distinguished by the location of the sections having the greatest blade width. It was found that the propeller blade with maximum chord length near the root had higher propulsive efficiency. However, the propellers used in this study had advance ratio mainly within the range of $1.0 < \lambda < 2.2$, for lower advance ratio range, the effect of blade planform variation on propeller performance is still remained questionable. Gur (2014) presented a semi-analytic method for estimating the maximal efficiency available for a propeller using the propeller integral properties (i.e., diameter, activity factor, or solidity) and the flight conditions which include the advance ratio and power coefficient. However, the influences of the chord length distribution and advance ratio on the aerodynamic performance were not discussed in his research.

In this study, five scaled HAA propellers that are distinguished by the chord length at tip are tested in a low speed wind tunnel. The influence of Reynolds number is firstly investigated through tests of one propeller at different rotational speeds. Then, these propellers are tested in the condition of $Re_{0.7}$ larger than the critical Reynolds number. The influences of advance ratio and blade planform on propeller aerodynamic performance, especially the propulsive efficiency, are illustrated according to the test results.

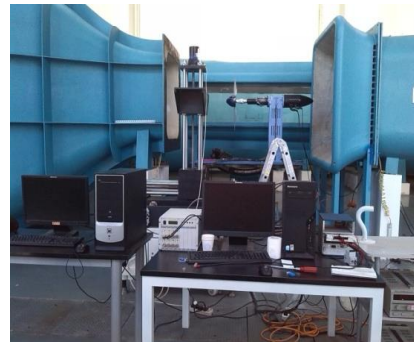
2. EXPERIMENT SETUP

2.1 Wind Tunnel

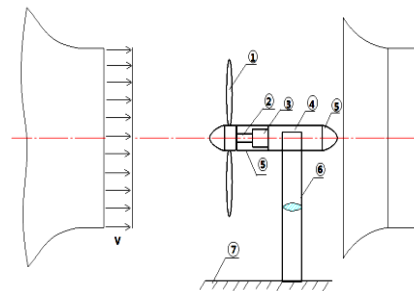
The tests are conducted in a low turbulence aeroacoustic wind tunnel (D5 wind tunnel) at Beijing University of Aeronautics and Astronautics (BUAA). It is an open cycle type wind tunnel (see Fig. 2a) with a test section size of $1 \text{ m} \times 1 \text{ m} \times 2.5 \text{ m}$ ($H \times W \times L$). The free-stream speed of test section is up to 80 m/s with turbulence intensity of less than 0.08%. In the present study, the $Re_{0.7}$ varied from 1.2×10^5 to 3.2×10^5 .

The experiment is arranged as shown in Fig. 2b. The propeller axis is fixed along the central line of the wind tunnel. The propeller is driven by a servo motor which is mounted on a streamline shaped steel strut and capable of delivering 5 KW power at 3000 rpm. In order to reduce the influence of

supporting objects on the airflow, the fairing is used along the central axis.



a) The BUAA D5 wind tunnel



b) Schematic drawing of test arrangement

1 Propeller	2 Force balance
3 Conductive slip ring	4 Servo motor
5 Fairing	6 Strut
7 Stand	

Fig. 2. Wind tunnel and setting up.

2.2 Test Models

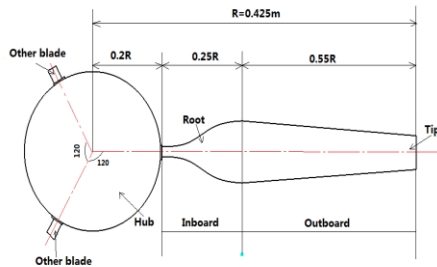
In order to investigate the influences of the blade planform and advance ratio, five blades (see Fig. 3a) which can be divided into two types, i.e., the narrow tip type ($b_{1.0}/b_{0.45} < 1$) and the wide tip type ($b_{1.0}/b_{0.45} \geq 1$), are designed. The narrow tip type includes the blades NTB-1, NTB-2 and NTB-3. The wide tip type includes the blades WTB-1 and WTB-2. Fig. 3b shows the conceptual drawing of one blade, from which it can be seen that the blade can be divided into two sections from tip to root, namely, the outboard and the inboard. The chord length distribution and blade twist angle distribution along radius of these five propellers are displayed in Fig. 3c. The chord length distribution of the inboard section ($0.25 \leq r/R \leq 0.45$) is the same for all these propellers. The chord length distribution of the outboard section ($0.45 \leq r/R \leq 1.0$) is different and linear with radius. The blade twist angle distribution of these five propellers is the same. In order to describe the blade planform, the parameter CR which is defined as $CR = b_{1.0}/b_{0.45}$ is introduced and given in Table 2. Other geometric parameters of each blade are also listed in this table. The diameter of all five propellers is 0.85 m. Each propeller consists of three blades. The airfoil is a typical low Reynolds number airfoil S1223, and the pitch angle is 20.5° ($r/R = 0.7$).

Table 2 Parameters of the blades

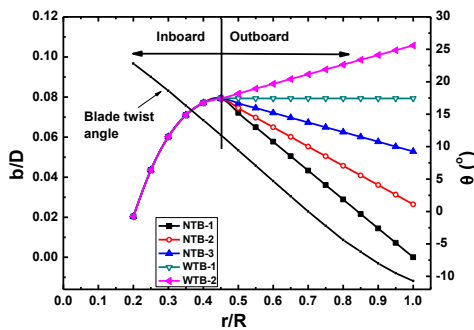
Type	Name	CR	$b_{0.7}/D$	AF	C/b	$\Delta\theta$	$\chi_{0.7}$
Narrow tip	NTB-1	0	0.043	43.4	0.12	32.8°	20.5°
	NTB-2	0.33	0.055	70.0	0.12	32.8°	20.5°
	NTB-3	0.67	0.067	96.6	0.12	32.8°	20.5°
Wide tip	WTB-1	1.00	0.079	123.2	0.12	32.8°	20.5°
	WTB-2	1.33	0.091	149.8	0.12	32.8°	20.5°



a) Photograph of blades



b) Conceptual drawing of one blade



c) Geometric parameters along radius

Fig. 3. Geometry of the blades.

2.3 Force Measurement

The thrust and torque are measured by a six-component strain-gauge balance. One end of the balance is connected to the propeller, and the other end is mounted on the shaft of the servo motor. A cylindrical conductive slip ring is fixed on the servo motor shaft to conduct the electric signals to the data acquisition system, which is consisted of an amplifier and an analog voltage acquisition card. The sample rate is 1,000 Hz and a total number of 60,000 samples are collected for each test case. The thrust coefficient, power coefficient and propulsive efficiency are calculated from the thrust, torque and velocity measured. The blockage effect is considered in the analysis program using the

management method described by Glauert (1926). The uncertainty of propulsive efficiency in these tests is less than 1.4%.

3. RESULTS AND DISCUSSION

3.1 Influence of Reynolds Number

Since the propeller with blade NTB-1 is most likely to be influenced by Reynolds number due to its smallest chord length and therefore lowest Reynolds number, it is selected and tested at two rotational speeds of 1500 rpm and 1850 rpm. The corresponding minimum Reynolds number $Re_{0.7}$ is 1.2×10^5 and 1.5×10^5 .

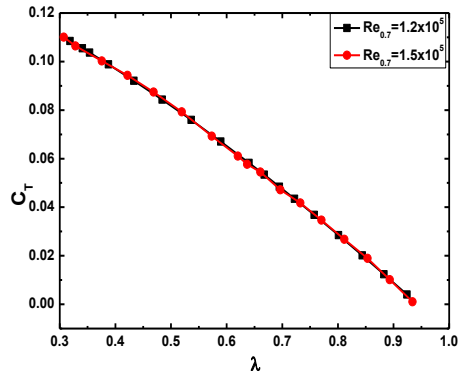
Figure 4 shows the performance curves of the propeller with blade NTB-1 at different Reynolds numbers. It can be seen that the curves of thrust coefficient, power coefficient and propulsive efficiency at different Reynolds numbers almost overlap, which indicates that the influence of Reynolds number on propeller performance is negligible when $Re_{0.7}$ is above 1.2×10^5 . The following tests of each propeller are carried in the condition of $Re_{0.7} \geq 1.5 \times 10^5$.

3.2 Effect of Chord Length Distribution on Aerodynamic Performance

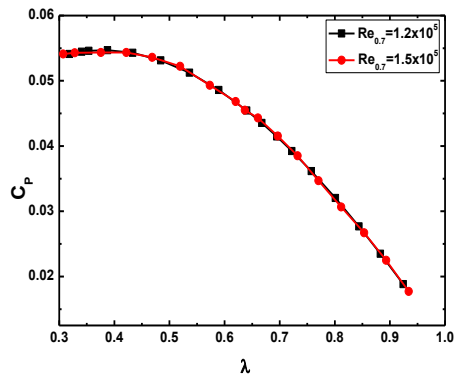
3.2.1 Aerodynamic Performance against Advance ratio

The thrust coefficients, power coefficients and propulsive efficiencies of these propellers at the rotational speed of 1850 rpm are displayed respectively in Fig. 5. With the increasing advance ratio, both the thrust coefficients and power coefficients of these propellers decrease gradually. The thrust coefficients approach to zero in the large advance ratios of $\lambda = 0.93 - 0.98$, which is also called ‘zero-thrust state’. As shown in Fig. 5, at the same advance ratio, both the thrust coefficient and power coefficient increase with CR.

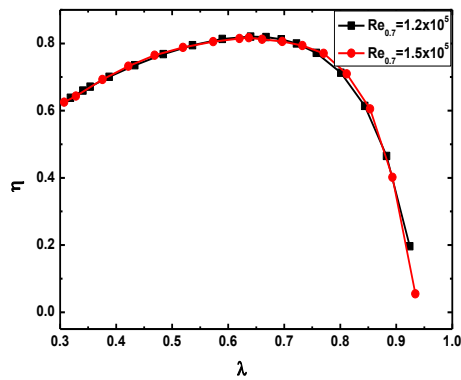
For all propellers, with the increasing advance ratio, the propulsive efficiencies first increase slowly to the maximum values at the advance ratios of $\lambda = 0.64 - 0.72$, and then drop quickly to nearly zero at the advance ratios of $\lambda = 0.93 - 0.98$. It can be also observed that these five efficiency curves cross at the critical advance ratio of about $\lambda = 0.8$, which divides the efficiency curves into two regions: the low advance ratio region ($\lambda < 0.8$) and the high advance ratio region ($\lambda > 0.8$). In the low advance ratio region, the propulsive efficiency decreases with CR. In the high advance ratio region, the propulsive efficiency increases with CR.



a) Thrust coefficients

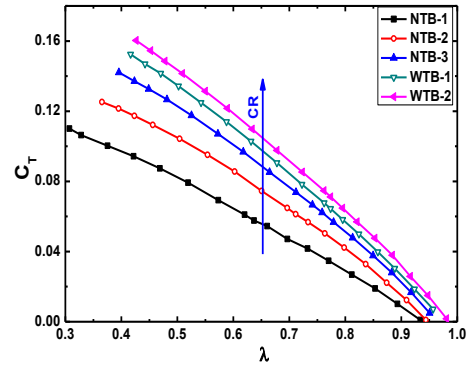


b) Power coefficients

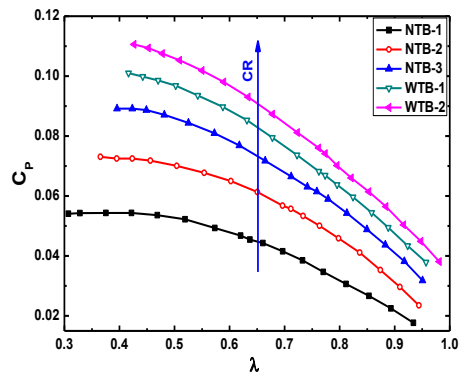


c) Propulsive efficiencies

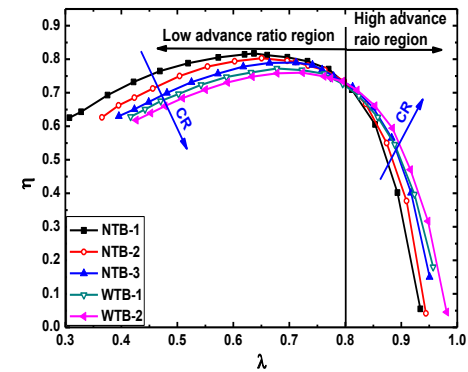
Fig. 4. Aerodynamic performance of the propeller with the blade NTB-1 at different $Re_{0.7}$.



a) Thrust coefficients



b) Power coefficients



c) Propulsive efficiencies

Fig. 5. Aerodynamic performance of these five propellers.

3.2.2 Influences of the Blade Planform and Advance Ratio on Propulsive Efficiency

According to the propeller strip theory presented by Liu (2006) and Liu *et al.* (2011), the airflow around a blade element at radius r is displayed in Fig. 6, in which φ_0 is the local airflow angle, α is the blade element attack angle and β is the interference angle.

a) Thrust coefficients a) Thrust coefficients

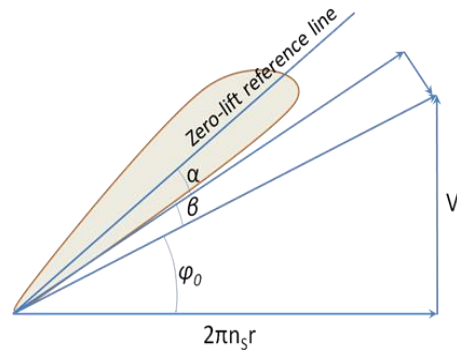


Fig. 6. Diagram of blade element and airflow.

The local blade element efficiency η is expressed as

$$\eta = \frac{\tan \varphi_0}{\tan(\varphi_0 + A)} \quad (3)$$

Where $A = \beta + \gamma$. The blade element efficiencies at different A are plotted against φ_0 in Fig. 7.

From Fig. 7, for a fixed A , with the increasing airflow angle, the blade element efficiency first increases rapidly. Then, it keeps a high value within the wide range of $15^\circ < \varphi_0 < 70^\circ$. Finally, the blade element efficiency begins to drop rapidly when $\varphi_0 > 70^\circ$. At the same φ_0 , the blade element efficiency decreases with the increase of A . For convenience, the efficiency curves are generally divided into three regions: the low efficiency region of blade tip ($\varphi_0 < 15^\circ$), the middle high efficiency region ($15^\circ < \varphi_0 < 70^\circ$) and the low efficiency region of blade root ($\varphi_0 > 70^\circ$). The analysis of propulsive efficiency can be carried from Fig. 7.

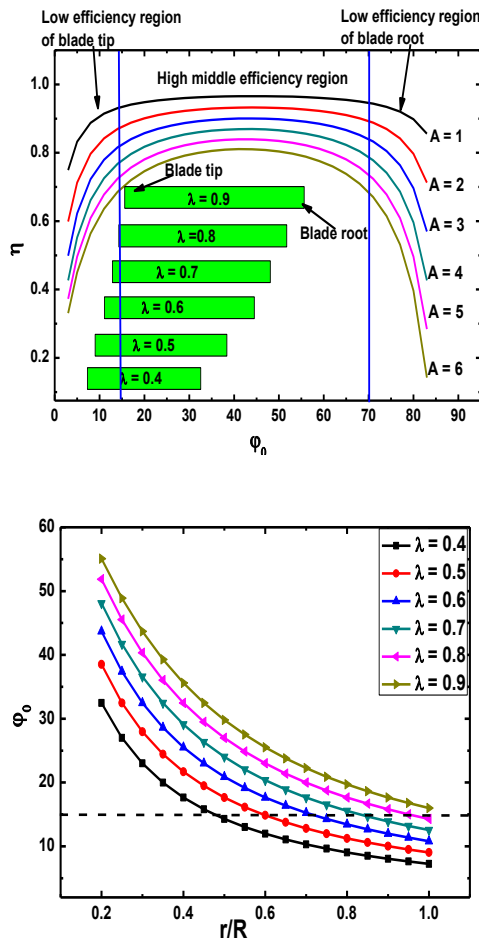


Fig. 8. Airflow angle along radius at different advance ratios.

According to the definition, the φ_0 in Eq. 3 is expressed as

$$\varphi_0 = \arctan\left(\frac{V}{2\pi n_s r}\right) = \arctan\left(\frac{\lambda R}{\pi r}\right) \quad (4)$$

The distributions of φ_0 along radius at different advance ratios are displayed in Fig. 8. It can be seen that the φ_0 decreases with radius for a given advance ratio and increases with advance ratio at a given radius r . For convenience, the ranges of φ_0 at different advance ratios are also displayed in the below of Fig. 7.

The A in Eq. 3 is determined by γ and β . The γ is mainly influenced by the airfoil, blade element attack angle and Reynolds number. The β can be solved with the equation as below (Weick 1930).

$$\frac{N_B b}{2\pi r} C_L = \frac{4 \sin(\varphi_0 + \beta) \tan \beta}{1 - \tan \gamma \tan \beta} \quad (5)$$

From Eq. 5, the β at radius r is influenced by the local chord length b , airflow angle φ_0 , lift coefficient C_L and drag-lift angle γ . Since the main concern is the chord length at tip, the influences of φ_0 and chord length (CR) on β are calculated in the conditions of $r = R$, $\gamma = 1$ and $C_L = 0.5$ and displayed in Fig. 9. It can be seen that, at blade tip, the β increases with the chord length and decreases with φ_0 .

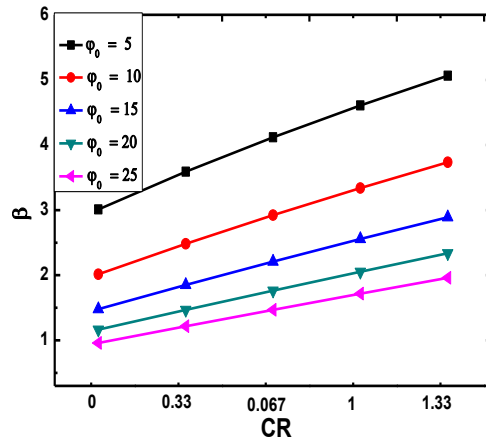


Fig. 9. Interference angle at different airflow angles.

As shown in Fig. 7, the low φ_0 and large A are the direct causes that lead to the low blade element efficiency. When the advance ratio is below 0.8, because the φ_0 of tip is below 15° as shown in Fig. 8, the blade tip has entered into the low efficiency region as shown in Fig. 7. For the A ($A = \beta + \gamma$), because the airfoil is the same for these propellers and the influence of Reynolds number is negligible in the tests, the γ is the same for each propeller at the blade element attack angle of maximum lift-drag ratio. The β of wider blade is larger than that of narrower blade as shown in Fig. 9, making the A of the wider blade larger than that of the narrower blade. Hence, the blade element efficiency of the wider blade is lower than that of the narrower blade, which results in the lower propulsive efficiency for the propellers with wide tip as shown in Fig. 5c.

When advance ratio is larger than 0.8, as shown in Fig. 7, the blade elements efficiency of tip are within the high middle efficiency region. For the A ,

the increase of the ϕ_0 makes the difference of β between the wider and narrower blade to become to be very small as shown in Fig. 9. The γ at radius r is the same for these propellers as mentioned. Hence, the difference of A between the wider and the narrower blade propellers becomes to be very small, which results in the influence of A to be a less important factor. In this case, increasing the chord length of blade tip means more proportion of load will be taken by the tip, which is favorable to the propulsive efficiency for the wider blade propeller as shown in Fig. 5c.

In summary, both theoretical analysis and experimental results show that, for the large thrust and low advance ratio ($\lambda < 0.8$) HAA propellers, the blade with narrow tip is favorable to the propulsive efficiency. For the HAA propellers with high advance ratio ($\lambda > 0.8$), the blade with wide tip is favorable to the propulsive efficiency.

4. CONCLUSIONS

Wind tunnel tests of five scaled HAA propellers which are distinguished by tip chord length are carried. The influences of Reynolds number, blade planform and advance ratio on propeller aerodynamic performance are discussed according to the experimental results. The following conclusions can be made.

- 1) For the propeller with airfoil S1223, the influence of Reynolds number is negligible when $Re_{0.7}$ is above 1.2×10^5 .
- 2) When the advance ratio is below 0.8, decreasing the chord length at tip is favorable to the propulsive efficiency because the blade elements are in the low efficiency region. It is suggested that the blade with narrower tip should be adopted by the large thrust and low advance ratio HAA propellers.
- 3) When the advance ratio is above 0.8, for that the blade elements of tip are in the high efficiency region, the propeller propulsive efficiency can be benefitted by increasing the tip chord length. Therefore, the blade with wide tip should be adopted by the high advance ratio HAA propellers.

In the future, the influence of pitch angle will be studied.

ACKNOWLEDGMENTS

This work was partially supported by the National Natural Science Foundation of China (No.11302015, 11272034).

REFERENCE

Alam, M. I. and R. S. Pant (2013). A Methodology for Conceptual Design and Optimization of a High Altitude Airship. *AIAA Lighter-Than-Air Systems Technology (LTA) Conference*.

Bass, R. (1986). Small scale wind tunnel testing of

model propellers. *Aerospace Sciences Meeting, 24th, Reno, NV*.

Beemer JD, P. R., L. L. Rueter and P. A. Seuferer (1975). POBLA-S, The Analysis and Design of a High Altitude Airship. *DTIC Document*.

Borst, H. V. (1973). Summary of Propeller Design Procedures and Data. Aerodynamic Design and Installation. *DTIC Document*.

Borst, H. V. (1973). Summary of Propeller Design Procedures and Data: Structural analysis and blade design. *National Technical Information Service, US Department of Commerce*.

Brandt, J. B. (2005). *Small-scale propeller performance at low speeds*, University of Illinois at Urbana-Champaign.

Brandt, J. B. and M. S. Selig (2011). Propeller performance data at low Reynolds numbers. *49th AIAA Aerospace Sciences Meeting*.

Brooke, L. (2005). High altitude LTA platforms: capabilities and possibilities. *AIAA 5th Aviation, Technology, Integration, and Operations Conference (ATIO), Arlington, Virginia*.

Colozza, A. J. (2003). Comparison of Mars Aircraft Propulsion Systems. *NASA/CR—2003-212350*.

Glauert, H. and C. Lock (1926). On the advantages of an open jet type of wind tunnel for airscrew tests. *DTIC Document*.

Gur, O. (2014). Maximum Propeller Efficiency Estimation. *Journal of aircraft* 51(6).

Hartman, E. P. and D. Biermann (1938). The aerodynamic characteristics of four full-scale propellers having different planforms. *NACA-report, 643*.

Kim, D. M. and *et al.* (2003). Korea stratospheric airship program and current results. *AIAA Paper 6782*.

Koch, L. D. (1998). Design and performance calculations of a propeller for very high altitude flight. *Case Western Reserve University*.

Liu, P. Q. and *et al.* (2011). Ground wind tunnel test study of the propeller of stratospheric airships. *Journal of Aerospace Power* 26(8), 1775-1781.

Liu, P. (2006). *Theory and Application of Airscrews*, Beihang University Press (in Chinese), Beijing.

Liu, P. and *et al.* (2011). Aerodynamics properties and design method of high efficiency-light propeller of stratospheric airships. *Remote Sensing, Environment and Transportation Engineering (RSETE) International Conference on, IEEE*.

Merchant, M. P. and L. S. Miller (2006). Propeller performance measurement for low Reynolds number UAV applications. *AIAA 1127*.

Mikkelsen, D. C. and *et al.* (1984). Summary of

- recent NASA propeller research. *NASA Technical Memorandum*.
- Mueller, J. B. and *et al.* (2004). Development of an aerodynamic model and control law design for a high altitude airship. *DTIC Document*.
- Okuyama, M. and *et al.* (2006). Study of propulsion performance and propeller characteristics for stratospheric platform airship. *Japan Aerospace Exploration Agency*.
- Pancotti, A. (2009). An overview of advanced concepts for near-space systems. *45th AIAA Joint Propulsion Conference and Exhibit*.
- Schmidt, D. K. and *et al.* (2007). Near-space station-keeping performance of a large high-altitude notional airship. *Journal of Aircraft* 44(2), 611-615.
- Smith, I. and M. Lee (2007). The hisentinel airship. *AIAA 7748*.
- Weick, F. E. (1930). *Aircraft propeller design*, McGraw-Hill Book Company, inc.

